Cold atoms in cranked ring lattices.*

A. F. R. de Toledo Piza
Departamento de Física Matemática,
Instituto de Física, Universidade de São Paulo,
C.P. 66318, 05315-970 São Paulo, S.P., Brazil

March 17, 2008

Abstract

The dynamics of cold bosons in a periodic one-dimensional rotating ring lattice is treated in a representation constructed in terms of first band Bloch functions. This is essentially equivalent to the quasi-momentum representation of the usual Bose-Hubbard model in the limit of strong lattice potentials (small hopping term), but incorporates additional effects via Bloch single particle energies in the case of large hopping. Extension to rotating ring lattices is straightforward. Bose-Einstein condensation phenomena associated with the Mott transition under lattice rotation and the corresponding condensate wavefunctions are obtained in a many-body framework. The use of correct lattice single particle energies is found to cure an inconsistency which occurs in the usual Bose-Hubbard model ground state inertial parameters used to define superfluid fractions in the phenomenological two-fluid picture.

1 Introduction

The dynamics of N cold bosonic atoms in an external lattice trap is currently modelled in terms of the Bose-Hubbard hamiltonian

$$H_{\rm BH} = -J \sum_{<i,j>} (a_i^\dagger a_j + a_j^\dagger a_i) + \sum_i \epsilon_i a_i^\dagger a_i + \frac{U}{2} \sum_i a_i^\dagger a_i^\dagger a_i a_i, \qquad J,\ U > 0 \tag{1}$$

where the first term describes nearest neighbour hopping, the second term accounts for the different site energies due to the presence of the slowly varying overall trap potential to which the finer periodic structure is superimposed and the last term accounts for on-site effective two-body repulsion. This hamiltonian can be heuristically derived[1] by using, as a

*Prepared for ccm08, MPIPKS, Dresden, March 5-8 2008.

representation, lattice Wanier functions for the first band in order to introduce localisation and to provide for reasonable truncation of the more general field hamiltonian

$$H = \int d^3r\ \psi^\dagger(\vec{r}) \left(-\frac{\hbar^2\nabla^3}{2m} + V_{\rm trap}(\vec{r}) + \frac{\lambda}{2}\psi^\dagger(\vec{r})\psi(\vec{r}) \right) \psi(\vec{r}), \tag{2}$$

where $\lambda \equiv 4\pi\hbar^2 a/m$ plays the role of the strength of an effective, zero range two-body interaction. The fact that it is expressed in terms of the atom-atom scattering length a signals that it is an object possessing the hierarchy of the two-body scattering amplitude, as e.g. in Brueckner theory[2]. This is in fact a crucial feature for proving depletion free Bose-Einstein condensation (for purely repulsive two-body potentials) in the extreme 'dilute' Gross-Pitaevski limit defined by Lieb and Seiringer[3],[4] as $N \to \infty$, $a \to 0$ with Na constant. Sufficiently close to this limit, the physics of the condensate is describable in terms of a single mode, which can be obtained as the minimiser of the Gross Pitaevski functional constructed in terms of the field hamiltonian H, providing for a solid basis for the reach of the Gross-Pitaevski equation, whenever the connecting lifeline is not too long or fragile[5]-[7].

Cold atoms in lattice potentials at low mean occupation per site, on the other hand, involve necessarily a many-mode situation, to which the many-body character of the Bose-Hubbard model becomes relevant. The salient physics here hinges on a quantum phase transition between between a 'Mott insulator' and a 'superfluid' phase, which involves many-body correlation phenomena resulting from competition between localisation, favoured by two-body repulsion, and delocalization, favoured by the hopping term. It can be exposed in very simple terms[8] for the case of of a one-dimensional, uniform, boundless (periodic) lattice with M sites, corresponding to a ring-like geometry[9]. This dispenses, in particular, with the rather more heuristic local one body term of the Bose Hubbard Hamiltonian (1). The hopping term is diagonalized by transforming to the quasi-momentum operators

$$A_q \equiv \frac{1}{\sqrt{M}} \sum_{n=1}^{M} e^{\frac{2\pi i}{M}nq} a_n, \qquad q = 0, \ldots, M-1, \tag{3}$$

so that the hamiltonian becomes

$$H_{BH} \to -2J \sum_{q=0}^{M-1} \cos\left(\frac{2\pi q}{M}\right) A_q^\dagger A_q + \frac{U}{2M} \sum_{q_j} \delta_M(q_1+q_2-q_3-q_4) A_{q_3}^\dagger A_{q_4}^\dagger A_{q_2} A_{q_1} \tag{4}$$

where the modular Kronecker delta $\delta_M(q)$ is equal to one if $q = 0, \pm M, \pm 2M, \ldots$ and zero otherwise. This shows that, in addition to the total number of bosons $N \equiv \sum_n a_n^\dagger a_n \equiv \sum_q A_q^\dagger A_q$, the total quasi-momentum is also a (modular) constant of motion and can be used to label eigenstates[10]. This reveals as an extra bonus the fact that the one-body density of the good total quasi-momentum eigenstates, which plays a crucial role in the general Penrose-Onsager characterisation of Bose-Einstein condensation[11], is diagonal in the quasi-momentum representation. Elementary perturbative methods on the two extreme

cases $J \to 0$, $U > 0$ and $J > 0$, $U \to 0$ suffice to reveal the structure of the 'ground state phase diagram'[12] which plots scaled ground state energy differences $(E_{N+1} - E_N)/U$ against J/U. It reduces to negative slope parallel lines whose separation is $1/M$ at the extreme right hand side (very large values of J/U) which bunch together in groups of N lines at $J/U = 0$, making room for the (in this case, cf. ref.[13]) elongated Mott insulator 'lobes' (see e.g. fig. 2), and clearly indicating a cleavage of the diagram.

Considerations involving rotating containers in general, and rotating ring lattices in particular, are theoretically relevant[14, 15] for assessing superfluidity properties of cold atom systems. Work along this line has been recently reported by Oktel et al., using the Bose-Hubbard hamiltonian for a two-dimensional rotating lattice and either a mean-field approximation[16] or Gutzwiller type variational wavefunctions[17]. An alternative approach to superfluid properties, used in connection with one-demensional lattices, involves treating the time evolution of prepared 'supercurrent states'[18]. In this presentation I will discuss some results for the rotating ring lattice in which, instead of stressing localisation while allowing for hopping, as in the Bose-Hubbard hamiltonian, a more standard representation-truncation scheme is used making direct use of the Bloch functions for the first band. This provides in particular for an explicit set of single-boson wavefunctions (modes) labelled by a quasi-momentum quantum number, with an associated set of single-boson energies. As in the case of eq.(4), the one-body part of the truncated field hamiltonian (2) is diagonal, and total Bloch quasi-momentum is (modularly) conserved. Cranking of the ring lattice can be dealt with in a straightforward way, allowing in particular for the calculation of system parameters related to superfluid flow in the system. The resulting problem can easily be handled in terms of numerical diagonalization in the case of not too many sites and few particles per site.

2 Cranked quasi-momentum hamiltonian

The following discussion is based on the cranked one-dimensional version of the field hamiltonian (2) obtained by assuming that the degrees of freedom transverse to the lattice ring with M sites, lattice parameter b and radius $R = Mb/2\pi$ are frozen and/or decoupled. Using as relevant variable the azimuthal angle φ,

$$H_{\rm Ring} = \int d\varphi \;\; \psi^\dagger(\varphi) \left[\frac{1}{2mR^2} \left(\frac{\hbar}{i} \frac{d}{d\varphi} - mR^2\omega \right)^2 + V_{\rm latt}(\varphi) + \frac{\Lambda}{2} \psi^\dagger(\varphi)\psi(\varphi) \right] \psi(\varphi) \qquad (5)$$

where ω is the cranking angular velocity and Λ is the effective longitudinal two-body interaction parameter. The lattice potential satisfies $V_{\rm latt}(\varphi) = V_{\rm latt}(\varphi + 2\pi/M)$, so that the one-body part of (5) can be diagonalized in terms of Bloch eigenfunctions

$$\phi_q^{(\omega)}(\varphi) = \frac{1}{\sqrt{2\pi}} e^{iq\varphi} u_{\kappa_q}^{(\omega)}(\varphi), \quad q = 0, 1, \ldots, M-1, \quad u_{\kappa_q}^{(\omega)}(\varphi) = u_{\kappa_q}^{(\omega)} \left(\varphi + \frac{2\pi}{M} \right)$$

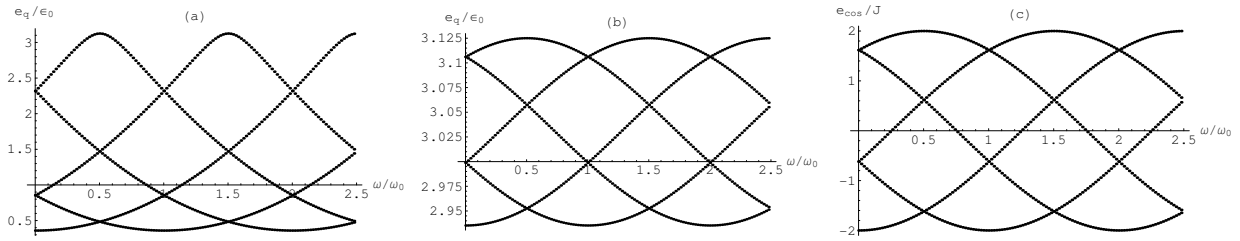

Figure 1: (a) and (b): First band Bloch single particle energies, for $M = 5$, $\gamma = \hbar^2/mR^2$ and $100\,\hbar^2/mR^2$ respectively, as functions of the cranking angular velocity ω/ω_0; (c): Bose-Hubbard single-particle energies per unit hopping parameter also as a function of ω/ω_0. Note the relative compression of lower levels in the case of the smaller value of γ. The ratio of the width of the Bloch band to that of graph (c) may be used to associate an effective Bose-Hubbard hopping parameter J to each value of γ. The values of J for (a) and (b) are $J = 0.41\,\hbar\omega_0$ and $J = 0.019\,\hbar\omega_0$ respectively.

with single particle eigenvalues $e_q^{(\omega)}$. Using the Bloch functions to define creation and annihilation operators $A_q^{(\omega)\dagger}$, $A_q^{(\omega)}$ and truncating to the first band one obtains the cranked quasi-momentum hamiltonian

$$H_q^{(\omega)} = \sum_{q=0}^{M-1} e_q^{(\omega)} A_q^{(\omega)\dagger} A_q^{(\omega)} + \frac{1}{2} \sum_{q_i} \Lambda_{\{q_i\}}^{(\omega)} \delta_M(q_1 + q_2 - q_3 - q_4) A_{q_1}^{(\omega)\dagger} A_{q_2}^{(\omega)\dagger} A_{q_4}^{(\omega)} A_{q_3}^{(\omega)}. \qquad (6)$$

The 'two-body matrix elements' $\Lambda_{\{q_i\}}^{(\omega)}$ involve integrals of four Bloch functions with modular conservation of total quasi-momentum made explicit by the Kronecker delta δ_M.

Relevant properties of this hamiltonian can be illustrated by adopting a schematic realization (of the Kronig-Penney type) of the lattice potential as

$$V_{\rm latt} \to \gamma \sum_{n=0}^{M-1} \delta\left(\varphi - \frac{2\pi}{M}(n + 1/2)\right),$$

for which Bloch functions and single-particle (quasi-momentum) energies can be easily obtained explicitly. The latter are shown in fig. 1 as functions of the cranking angular velocity ω/ω_0, $\omega_0 = \hbar/mR^2$, for two different values of γ. For comparison, the values of $-2\cos\left(\frac{2\pi}{M}(q - \frac{\omega}{\omega_0})\right)$, $q = 0, \ldots, M$, which correspond to the one-body term of the standard Bose-Hubbard hamiltonian (4) when $\omega = 0$, are also shown. This cosine function reproduces the relative spacings of the single-particle energies very accurately for sufficiently large values of γ, while there is a clear low-energy bunching of the single particle levels for the lower values. The effect of the cranking angular velocity on the single-particle energies is seen to consist of a rotation which leads to single-particle level crossings at integer and half-integer values of ω/ω_0. In particular, the quasi-momentum of the lowest level increases by one at half-integer values.

On the basis of this, an effective hopping parameter J may be obtained as the ratio of the width of the first band to the full range 4 of its cosine function ersatz. This value of J will be used from here on as a substitute for γ whenever use is made of the Bloch single-particle energies, as this allows for a more direct comparison with results using the standard Bose-Hubbard quasi-momentum energies, as they appear in the hamiltonian (4). For sufficiently small J values both sets of single-particle energies differ by little, after allowing for an overall γ dependent (hence effective-J dependent) energy shift.

The two-body term of the quasi-momentum hamiltonian (6) also involves integrals over four Bloch functions $\Lambda^{(\omega)}_{\{q_i\}}$. Since these integrals do not differ too much, over a relevant range of values of ω, from the integral of four Wanier functions divided by the number of sites M, the replacement $\Lambda^{(\omega)}_{\{q_i\}} \to U/M$ has been used for simplicity in the numerical work.

3 'Ground state phase diagram'

Particle addition energies can be obtained by numerical diagonalization of the quasi-momentum hamiltonian (6) at quite low computational effort, in cases involving not too many sites and not too large mean occupation per site, if one takes advantage of the decoupling of states with different total quasi-momentum. Sample results are shown in fig. 2. In the case $\omega = 0$ all ground states have total quasi-momentum zero, so that this is the only subspace involved in the calculation. This is no longer true in general for $\omega \neq 0$, however. The general result can be easily derived from perturbative calculations for very small and very large values of J/U. One finds that, for values of ω such that the ground state quasi-momentum is q, $0 \leq q \leq M-1$, the ground state total quasi-momentum is $[nq]_{\mathrm{Mod\ M}}$. Commensurate values of N, i.e. $n = 0$ always corresponds to zero total quasi-momentum. Thus, in addition to the number cleavage present in the $\omega = 0$ case, one gets also a total quasi-momentum cleavage as a result of the effects of ring rotation. Furthermore, the spacing of the different lines approaches $1/M$ as J/U increases. It should be noted that the simplicity of the derivation in the limit of large values of J/U depends on the assumption made regarding the two-body matrix elements.

At the values of ω corresponding to crossings of single-particle levels the quasi-momentum hamiltonian acquires an additional 'parity' symmetry emphasised in ref. [10]. Explicitly, in the level crossing at integer values of ω/ω_0 in which the lowest single-particle state has quasi-momentum q_0, substitution of quasi-momentum q by the 'conjugate' value $[M-q+2q_0]_{\mathrm{Mod\ M}}$, i.e.

$$A_q \to A_{[M-q+2q_0]_{\mathrm{Mod\ M}}}, \qquad \text{so that, in particular,} \qquad A_{q_0} \to A_{q_0},$$

leaves the hamiltonian invariant, since it also preserves the restrictions imposed by total quasi-momentum conservation in the two-body term. An analogous substitution rule exist for the level crossings at half-integer values of ω/ω_0, where the lowest single particle eigenvalue is degenerate. As a result of this symmetry, subspaces with different conjugate total quasi-momenta will give identical many-body energy spectra, and self-conjugate total

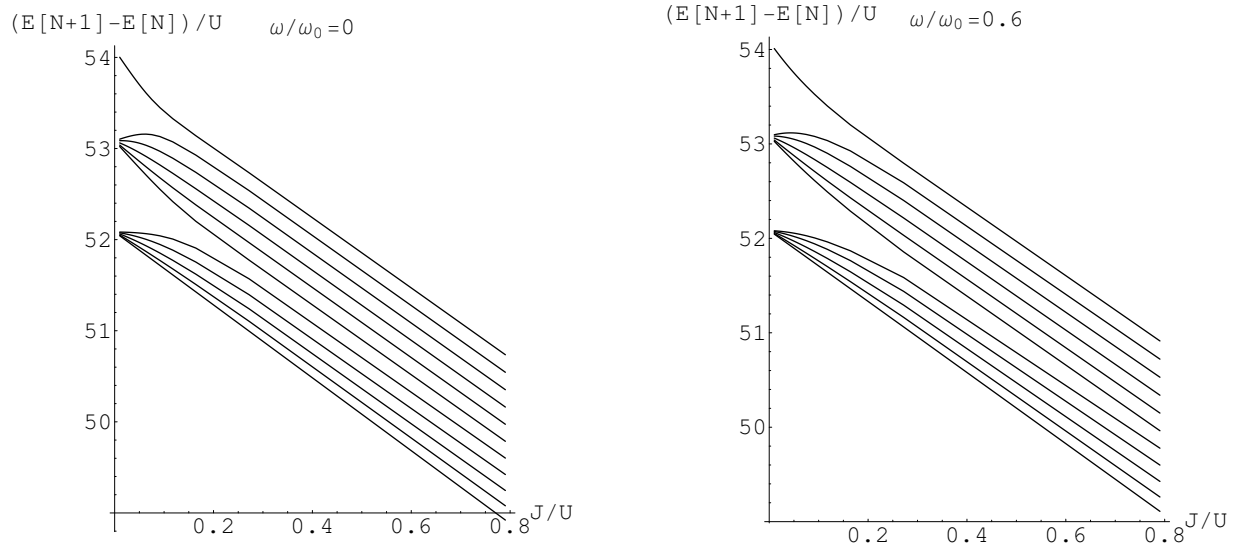

Figure 2: Particle addition energies as functions of J/U for $\omega = 0$ (left) and for $\omega = 0.6\,\omega_0$ (right) using Bloch s.p. energies, the effective hopping parameter defined in the text and a fixed value of $U = 0.06\,\hbar\omega_0$. In this case $M = 5$ and N varies from 0 to 11. The 'lobes' associated with the Mott transition are clearly seen. See text for details.

quasi-momentum subspaces can be further split into even and odd subspaces under quasi-momentum conjugation. Note again, however, that this symmetry is broken whenever the two-body matrix elements $\Lambda_{\{q_i\}}$ in (6) are themselves not invariant under quasi-momentum conjugation. Such invariance is of course valid 'a fortiori' under the assumption that all two-body matrix elements are equal.

The divergence, as J/U increases, of the M-fold bunches of lines in the extreme small hopping domain of the ground state phase diagram can also be easily estimated analytically. Since in this limit the spacings of the single-particle levels is very well described by the expression $-2\cos\left(\frac{2\pi}{M}(q - \frac{\omega}{\omega_0})\right)$, the perturbative slopes of the lines corresponding to $\mu_+ \equiv E[n_0M + 1] - E[n_0M]$ and $\mu_- \equiv E[n_0M] - E[n_0M - 1]$ are given by

$$\begin{aligned}
\frac{d(\mu_+/U)}{d(J/U)} &\rightarrow \frac{d(\Delta/U)}{d(J/U)} - 2(n_0+1)\cos\left[\frac{2\pi}{M}\left(q_+ - \frac{\omega}{\omega_0}\right)\right] + \mathcal{O}\left(\frac{J}{U}\right) \\
\frac{d(\mu_-/U)}{d(J/U)} &\rightarrow \frac{d(\Delta/U)}{d(J/U)} + 2n_0\cos\left[\frac{2\pi}{M}\left(q_- - \frac{\omega}{\omega_0}\right)\right] + \mathcal{O}\left(\frac{J}{U}\right),
\end{aligned}$$

where Δ is the overall J-dependent (and n_0-independent) energy shift of the single particle

energies and the $q_\pm$ are the quasi-momenta of the added/removed particle respectively. These expressions account for both the increase of the initial divergence of the bundles with n_0 and for its ω-dependent decrease, as seen in fig. 2.

4 Bose-Einstein condensation and condensate wavefunction

The fact that the ground many-body states have good total quasi-momentum implies that the corresponding one-body reduced densities are diagonal in the quasi-momentum representation, i.e.

$$\langle E[N]|A_q^{(\omega)\dagger}A_{q'}^{(\omega)}|E[N]\rangle = \rho_q^{(1)}\delta_{qq'}, \qquad \mathrm{Tr}\,\rho^{(1)} = N.$$

The corresponding eigenfunctions are the Bloch functions $\phi_q^{(\omega)}(\varphi)$. The onset of Bose-Einstein condensation is therefore signalled by eigenvalue dominance in this object, which also identifies the Penrose-Onsager condensate wavefunction[11] as one of the Bloch functions. Eigenvalue dominance always develops, as J/U increases, in the same scale as the closing of the 'lobes' associated with the Mott transition (see fig. 2).

As discussed in section 3 ground states for commensurate occupation (integer N/M) have total quasi-momentum zero for any ω, while in non-commensurate cases the ground state total quasi-momentum changes at the single-particle energy crossings occurring at half-integer values of ω/ω_0, so that the two cases are better dealt with separately.

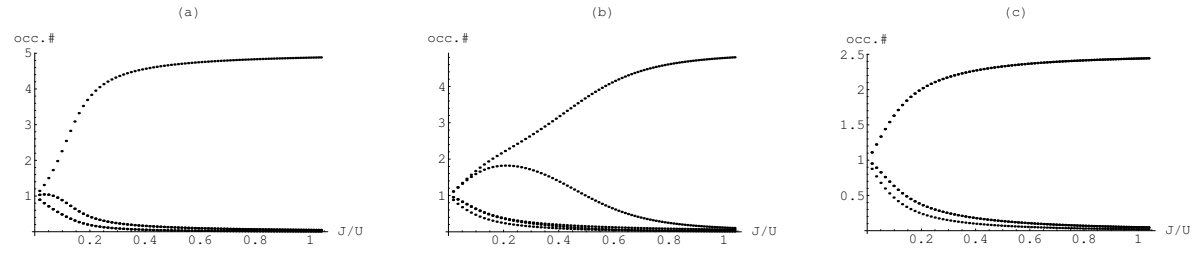

Figure 3: (a): Eigenvalues of the one-body density for $N/M = 1$, $M = 5$ and $\omega = 0$. The value of U has been again been fixed at $0.06\,\hbar\omega_0$. The largest eigenvalue corresponds to $q = 0$, and two lower eigenvalues, doubly degenerate due to the conjugation symmetry, correspond to $q = (1, 4)$ and $q = (2, 3)$ in decreasing order. (b) same for $q = 0, 1, 4, 2, 3$ (decreasing order) for $\omega/\omega_0 = 0.48$ and $q = 1, 0, 2, 4, 3$ for $\omega/\omega_0 = 0.52$. (c) same at the s.p. level crossing $\omega/\omega_0 = 0.5$, $q = (0, 1), (4, 2), 3$. Note the different scale graph (c).

In the commensurate case the eigenvalues of the ground state one-body density become fully degenerate in the limit of vanishing J/U, as a consequence of the repulsive character of the two-body effective interaction. Their behaviour as J/U increases depends on the value of ω/ω_0, as illustrated in fig. 3. At the single particle level crossings in which the lowest single particle eigenvalue is doubly degenerate one gets asymptotically the sharing of

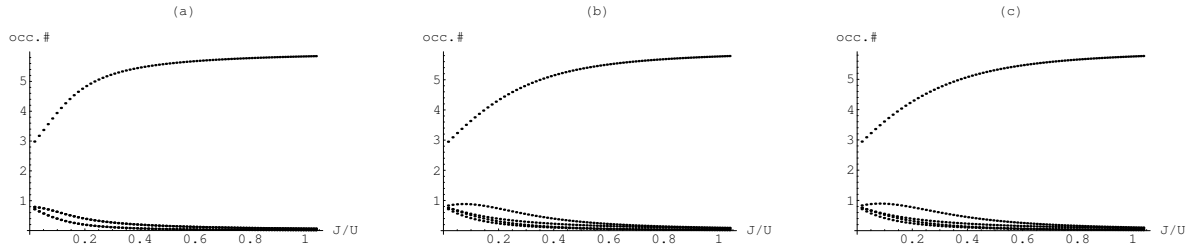

Figure 4: (a): Eigenvalues of the one-body density for $N/M = 1.2$, $M = 5$ and $\omega = 0$. The largest eigenvalue corresponds to $q = 0$, and two lower eigenvalues, doubly degenerate due to the conjugation symmetry, correspond to $q = (1, 4)$ and $q = (2, 3)$ in decreasing order. The total quasi-momentum is zero. (b) same for $q = 0, 1, 4, 2, 3$ (decreasing order), $\omega/\omega_0 = 0.48$, total quasi-momentum zero and $q = 1, 0, 2, 4, 3$, $\omega/\omega_0 = 0.52$, total quasi-momentum one. (c) same at the s.p. level crossing $\omega/\omega_0 = 0.5$, $q = 0, 1, 4, 2, 3$ for total quasi-momentum zero and $q = 1, 0, 2, 4, 3$ for total quasi-momentum one. In all cases $U = 0.06\,\hbar\omega_0$.

the total population between the two lowest orbitals, in the case of the many-body ground state (fig 3(c)). Fig. 3(b) indicates the behaviour of the occupation numbers as one moves away from the level crossing. For $\omega/\omega_0 = 1$ the occupations are again as in (a), but with $q = 1, (0, 2), (3, 4)$ in decreasing order of occupation number.

In the non-commensurate case, illustrated in fig. 4 for $N/M = 1.2$, the population sharing situation at the single particle level crossings does not occur, as the many-body ground states before and after the level crossing reside in different total quasi-momentum subspaces. Instead, in this case the many-body ground state becomes doubly degenerate for $\omega/\omega_0 = 0.5$. The two states can be chosen as having total quasi-momentum equal to each of the two values of the quasi-momenta of the lowest degenerate single particle levels, the corresponding asymptotic condensates carrying the full particle population N (fig. 4(c)). Moreover, the full degeneracy of the occupation numbers for vanishingly small values of J/U is no longer present due to the particle(s) which is (are) supernumerary to commensurability, together with the effect of bosonic enhancement factors. Note also the breaking of the double degeneracy of the orbitals with smaller occupation numbers in fig. 4(c). The breaking of the conjugation symmetry in this case is due to preferential occupation of one of the two lowest degenerate single-particle states in each of the two degenerate many-body ground states with sharp total quasi-momentum.

'Superfluid velocities', usually defined as the gradients of the phases of the condensate wavefunctions[15], may be immediately extracted from these results and from the appropriate Bloch functions. The transition from quasi-momentum zero to quasi-momentum one ground state condensate wavefunctions implies, in the model adopted in this calculation, a change from a 'librating' phase to a monotonically increasing phase. As seen from figures 3 and 4 this condensate wavefunction strongly dominates the one-body reduced density anywhere beyond the closure of the Mott 'lobes' (see fig. 2). The level crossings at commensurate occupation remain special cases in the sense that they are not 'protected' by a change also in the total quasi-momentum, leading to the previously mentioned double-condensate situations.

5 Ground state energy response to cranking

Superfluidity of the ground state of trapped, dilute Bose gases in the Gross-Pitaevski limit[3] has been demonstrated rather recently[4],[19] making use of a definition of the superfluid fraction of the system obtained from the ground state energy response to an externally imposed velocity field which is based on the phenomenological two-fluid model of superfluidity. For the toroidal geometry considered here this definition can be written as

$$\frac{1}{N}\left(E^{(\omega)}(N) - E^{(0)}(N)\right) = f_s \frac{1}{2} m R^2 \omega^2 + \mathcal{O}(\omega^4), \tag{7}$$

where $E^{(\omega)}(N)$ is the many-body ground state energy of the N particle system in the lattice reference system which rotates in the laboratory with the externally imposed angular velocity ω, and f_s is the superfluid fraction. This definition is motivated by the phenomenological two-fluid model, and interpreted accordingly as allowing for a fraction f_s of the mass of the system to remain at rest in the laboratory frame, while the remainder fraction, which corresponds to the 'normal' fluid, is carried around by the ring rotation. This interpretation requires therefore that $f_s < 1$.

Values for the quantity f_s defined in this way may be immediately extracted from the ω-dependence of many-body ground state energies obtained by diagonalizing the cranked quasi-momentum hamiltonian (6) or its counterpart in which the Bloch single-particle energies are replaced a cosine function properly scaled to the width of the first band by the effective

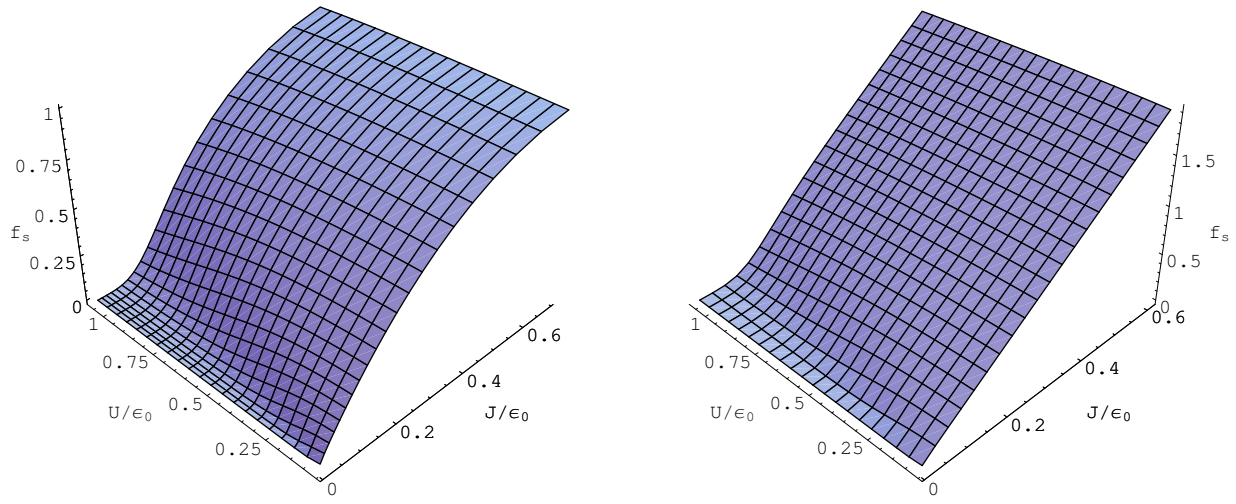

Figure 5: Superfluid fraction surfaces for Bloch s.p. energies (left) and Bose-Hubbard s.p. energies (right) over the $J \times U$ plane for $N/M = 1$. The energy unit is $\epsilon_0 = \hbar\omega_0$ as in previous figures. Note the different scales for f_s in the two cases. The inflection at the larger values of U is reduced for non-commensurate occupation, cf. fig. 6.

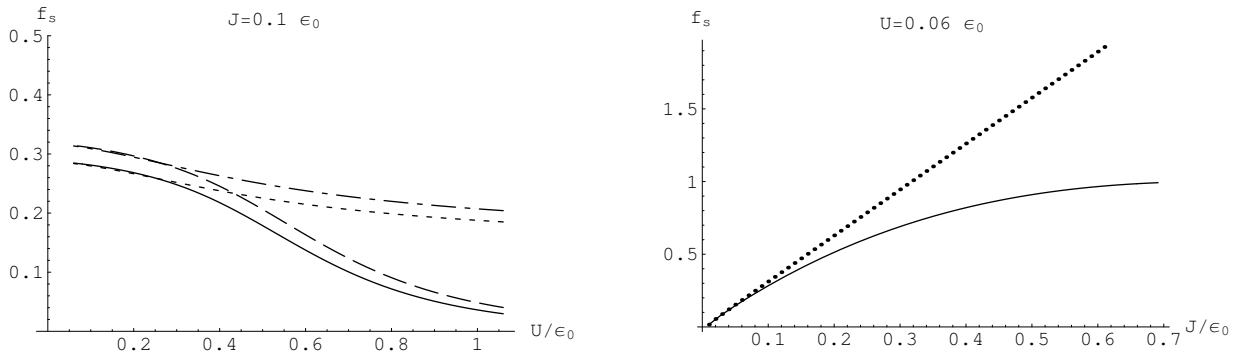

Figure 6: Cuts of the superfluid fraction surfaces for different sets of s.p. energies and commensurability. Left: Bloch s.p. energies (full line $N/M = 1$, short dashed line $N/M = 1.4$), Bose-Hubbard s.p. energies (long dashed line $N/M = 1$, long-short dashed line $N/M = 1.4$). Right: Bloch s.p energies (full line), Bose-Hubbard s.p. energies (dotted line), for both $N/M = 1$ and $N/M = 1.4$.

hopping coefficient J, which will be referred to as Bose-Hubbard single-particle energies. The results one obtains in each case are plotted in figs. 5 and 6. Since only small values of ω are involved, a simple perturbation calculation which takes into account the ω-dependence of the Bloch energies is in fact also adequate, although not used here. In fact, if one takes as the perturbation the term (neglecting the ω-dependence of the creation and annihilation operators)

$$\Delta H = \sum_{q=0}^{M-1} \left(e_q^{(\omega)} - e_q^{(0)} \right) A_q^\dagger A_q,$$

the perturbative energy shift is given directly in terms of the (diagonal) ground state one-body density $\rho^{(1)}$ in the Bloch quasi-momentum representation.

Fig. 5 shows surface plots of f_s as a function both of the two-body interaction parameter U and of the hopping coefficient J for the commensurate case $N/M = 1$, using Bloch single-particle energies and also using Bose-Hubbard single-particle energies. In the latter case one notably fails to obtain an expected saturation of $f_s \to 1$ as the value of J increases. It is worth stressing that, while Bose-Hubbard single-particle energy spacings closely approximate the Bloch energy spacings for J smaller than $\sim 0.02\,\hbar\omega_0$ (see fig.1), essentially all the range in which the saturation takes place lies beyond this limit.

Another relevant feature in the behaviour of the values of f_s is that it is strongly governed by the effective hopping parameter J with much weaker dependence on the two body interaction strength. Furthermore, it develops on a scale which is not related to the Bose-Einstein condensation as signalled by the eigenvalues of the single particle reduced density (cf. figs. 3 and 4). In fact, the onset of strong eigenvalue dominance is consistently found to be related to the closing of the Mott 'lobes' in the ground state phase diagram, where the obtained values of f_s are still far from saturation. The distinction between the condensate fraction,

in the sense of Penrose and Onsager[11], and the phenomenological concept of superfluid fraction is of course well known[20].

The effect of incommensurate occupation on the value of f_s is illustrated in fig. 6, which shows different cuts of the f_s surfaces both for $N/M = 1$ and for $N/M = 1.4$, also for both sets of single-particle energies, and consists basically in a reduction of the U-dependence of f_s which is apparent in the bending of the surfaces in fig. 5 at small J and large U. For the rather 'standard' value $U = 0.06\,\hbar\omega_0$ this is no longer noticeable.

6 Final remarks

Many features of the rich fenomenology of atomic Bose-Einstein condensates share the underlying simplicity of being amenable to theoretical treatment in terms of a single mode (or a few coupled modes in the case in which more than one species of boson is present) obeying nonlinear (coupled) dynamical equations derived in an effective mean-field framework. However, the Bose-Mott transition in an external potential lattice, which is most clearly discernible in situations involving small mean occupation per site, necessarily involves a many-mode situation. It presents thus the special challenge of treating correlations in a quantum many-body phase space. Possible single-mode dominance, as well as the characteristics of the dominant mode, appear as results in this context.

This work described an exploration of this type of system, in microscopic terms, in the simplest theoretical realization of a schematic rotating ring model. First band Bloch single-boson wavefunctions and energies are used, instead of the more often used Bose-Hubbard hamiltonian with constant next-neighbour hopping, without prejudice concerning quasi-momentum and parity symmetries (whenever applicable) of the latter model. The use of such symmetries provide for convenient tools for interpreting the results of the interplay of single particle and two-body interaction effects.

Rotation of the lattice ring gives access to quantities relevant for collective propensities such as the appearance of superfluid phases in the condensate wavefunction at different angular velocities and inertia parameters relevant for the two-fluid phenomenology of superfluidity. Superfluid fractions extracted from inertial parameters at low cranking angular velocities, using first band Bloch single-particle ingredients, are at least free of inconsistencies which occur with the standard Bose-Hubbard model. Both single-particle and many-body level crossings can be identified at the root of the changes of the system properties under variation of the external parameters.

Although the discussion has been limited here to properties of cranked ground states, the numerical availability of the full many-body spectrum allows for numerical calculation of the time evolution of non-stationary initial states essentially at no extra cost.

References

[1] D. Jaksch, C. Bruder, J. I. Cirac, C. W. Gardiner and P. Zoller, *Phys. Rev. Lett.* **81**, 3108 (1998).

[2] K. A. Brueckner and K. Sawada, *Phys. Rev.* **106**, 1117 and 1128 (1957); K. Sawada, *Phys. Rev.* **116**, 1344 (1959).

[3] E. H. Lieb and R. Seiringer, *Phys. Rev. Lett.* **88**, 170409 (2002).

[4] E. H. Lieb, R. Seiringer, J. P. Solovej and J. Yngvason, *The Mathematics of the Bose Gas and its Condensation*, Birkhuser Verlag, Base-Boston-Berlin (2005).

[5] B. Wu and Q. Niu, *Phys. Rev.* **A64**, 061603 (2001).

[6] L. Fallani, L. De Sarlo, J. E. Lye, M. Modugno, R. Saers, C. Fort and M. Inguscio, *Phys. Rev. Letters* **93**, 140406 (2004).

[7] A. Polkovnikov, E. Altman, E. Demler, B. Halperin and M. D. Lukin, *Phys. Rev.* **A71**, 063613 (2005).

[8] A. F. R. de Toledo Piza, *Braz. J. Phys.* **35**, 122.

[9] L. Amico, A. Osterloh and F. Cataliotti, arXiv:cond-mat/0501648.

[10] A. R. Kolovsky and A. Buchleitner, *Europhys. Lett.* **68**, 632 (2004).

[11] L. Penrose and L Onsager, *Phys. Rev.* **104**, 576 (1956).

[12] Matthew P. A. Fisher, Peter B. Weichman, G. Grinstein and Daniel S. Fisher, *Phys. Rev.* **B40**, 546 (1989).

[13] T. P. Polak and T. K. Kopeć, arXiv:cond-mat/0707.4383.

[14] A. J. Leggett, *Revs. Mod. Phys.* **73**, 307 (2001).

[15] A. J. Leggett, in *Bose-Einstein Condensation: from Atomic Physics to Quantum Fluids*, Proceedinge os the 13th. Summer School, edited by C. M. Savage and M. Das, World Scientific, Singapore (2000).

[16] M. Ö. Oktel, M. Nita and B. Tanatar, arXiv:cond-mat/0608350.

[17] R. O. Umcahlar and M. Ö. Oktel, arXiv:cond-mat/0704.2496.

[18] A. R. Kolovsky, *New Journal of Physycs* **8**, 197 (2006); *Pjys. Rev. Lett.* **99**, 020401 (2007).

[19] E. H. Lieb, R. Seiringer and J. Ynvason, *Phys. Rev.* **B66**, 134529 (2002).

[20] P. C. Hohemberg and P. C. Martin, *Ann. Phys.* (NY) **34**, 291 (1965).